CONF-791089--12

MASTER

NEUTRONS SCATTERING STUDIES OF THE ACTINIDES

by

G. H. Lander

Prepared for

International Magnetism Conference

Munich, Germany

September 3-7, 1979

U of C-AUA-USDOE

ARGONNE NATIONAL LABORATORY, ARGONNE, ILLINOIS

Operated under Contract W-31-109-Eng-38 for the

U. S. DEPARTMENT OF ENERGY

NEUTRON SCATTERING STUDIES OF THE ACTINIDES

G. H. Lander
Argonne National Laboratory*, Argonne, IL 60439 U.S.A.

Abstract

The electronic structure of actinide materials presents a unique example of the interplay between localized and band electrons. Together with a variety of other techniques, especially magnetization and the Mossbauer effect, neutron studies have helped us to understand the systematics of many actinide compounds that order magnetically. A direct consequence of the localization of $5f$ electrons is the spin-orbit coupling and subsequent spin-lattice interaction that often leads to strongly anisotropic behavior. The unusual phase transition in UO_2, for example, arises from interactions between quadrupole moments. On the other hand, in the monopnictides and monochalcogenides, the anisotropy is more difficult to understand, but probably involves an interaction between actinide and anion wave functions. A variety of neutron experiments, including form-factor studies, critical scattering and measurements of the elementary excitations have now been performed, and the conceptual picture emerging from these studies will be discussed.

Introduction

The most important single factor giving rise to the varied properties of actinides is the extended nature of the $5f$ electron wave functions. As a consequence of their spatial extent, the $5f$ electrons play a much greater role in bonding and related properties than the $4f$ electrons in the lanthanide series. At the same time the $5f$ electrons have an orbital component, $\ell = 3$,

that provides a potential for localization and such phenomena as a strong spin-lattice interaction. We might, therefore, expect properties ranging from that of itinerant $3d$ systems to that of localized $4f$ systems and, indeed, the literature of the actinides bears witness to a rich variety of magnetic behavior [1]. The new physics, however, seems likely to emerge from the examples of behavior intermediate between those of the other two major magnetic series, where existing theories can be tested in their limits.

In discussing experiments on transuranium materials everybody is aware, of course, of both the radioactivity and toxicity. In addition, large quantities of samples are seldom available, and neutron investigations are therefore at a disadvantage, since they often require at least 1 gram, and, for complex experiments involving inelastic scattering or polarization analysis, considerably more. Thus, no neutron experiments have been performed with elements heavier than curium and this seems unlikely to change within the next few years On the other hand, since neutrons easily penetrate most materials, once the actinide sample is encapsulated in a vanadium, aluminum, or even steel container, then the experiment is no more difficult than on any other system.

The Elements

The extension of the wave functions in the elements leads to direct exchange effects that result in a number of complex crystallographic phases for each element and almost magnetic behavior for U, Np, and Pu [1]. For some time the idea that a spin-density wave occurred at 40 K in alpha-uranium was fashionable, but recently at Oak Ridge National Laboratory careful measurements of the phonon spectra [2] led to the discovery of a charge-density

wave as responsible for the many anomalies at low temperature [3]. Since we are confining our attention to magnetic phenomena, we shall not describe this in detail, but the efforts do represent a major achievement for neutron scattering in view of the great many studies undertaken on α-U. The first element that exhibits spontaneous magnetic order is curium, as shown by Fournier *et al.* [4] by neutron diffraction. Unfortunately, this first experiment was not able to provide a solution to the antiferromagnetic structure of the metal, so that another experiment should be attempted.

Localization of 5*f* Electrons in Neptunium Compounds

Some years ago Hill [5] noticed that for many actinide compounds the occurrence of magnetic order could be correlated with a critical actinide-actinide separation (d_{An}). An excellent example of the validity of these ideas can be found in a series of neptunium Laves phase compounds, which have been examined by magnetization, Mossbauer, and neutron techniques [6,7]. A relationship must be found between the hyperfine field, H_{hf}, measured by the Mossbauer technique, and the magnetic moment μ_N, measured by neutron diffraction. Empirically a remarkably good linear relationship [8] exists between these two quantities and is shown in Fig. 1. This may be taken as strong evidence for localized 5*f* electrons, and it is also significant that the best fit extrapolates through the theoretical values for Np^{3+} ($5f^4$). However, as the moment becomes smaller we would not expect this relationship to continue to hold. A study of the compounds $NpAl_2$ (d_{An} = 3.37 Å) and $NpOs_2$ (d_{An} = 3.26 Å) showed this very clearly [7]. The idea quite simply is that as the actinide ions are brought closer together in, for example, $NpRu_2$ (d_{An} = 3.23 Å), the 5*f* electrons bandwidth increases until it is too wide to support spontaneous ordering. In $NpOs_2$ the moment is only 0.3 μ_B/Np

atom and a comparison of the magnetization, Mossbauer, and neutron experiments led to the conclusion that it was an itinerant system with extended $5f$ wave functions. Further confirmation of the itinerant nature of the magnetism in $NpOs_2$ comes from specific heat measurements [9].

Spin Lattice Interactions in UO_2

Uranium dioxide was one of the first actinide materials studied in detail by neutron scattering. Frazer, et al. [10] discovered the first-order phase transition from the paramagnetic to antiferromagnetic state, but the electronic structure remained in some doubt until the calculations of Rahman and Runciman [11] showed that the Γ_5 triplet of the predominant $^3H_4$ state was the ground state. Confirmation of this came from infra-red spectroscopy [12] and neutron inelastic scattering [13]. Attempts to fit the magnon dispersion curves with a conventional exchange coupled two-sublattice model were only qualitatively successful. The effect of introducing quadrupole-quadrupole interactions [12] gave excellent agreement, so that in a system like UO_2 with a large orbital ground-state degeneracy, the spin-lattice interaction leads to indirect quadrupole-quadrupole interactions that may be as strong as the exchange terms. One consequence of Allen's theory [12] was that the two oxygen sublattices should move with respect to each other. In 1974 we performed a careful neutron experiment at Argonne to measure the magnetic form factor and thereby attempt to identify the ground-state wave function (see below). To our surprise, a subset of the supposedly magnetic reflections appeared to get stronger with increasing Q ($= 4\pi \sin\theta/\lambda$, where θ is the Bragg angle and λ the neutron wavelength). After a thorough analysis this

subset of reflections was found to contain additional scattering from an internal rearrangement mode involving the oxygen sublattices [14]. The oxygen atoms shift by 0.014 Å from their special positions in the fluorite structure, see Fig. 2. The uranium lattice remains undisturbed, that is why we call the deformation an "internal distortion". Allen [12] was almost right, except that it is a transverse optic zone boundary mode that condenses rather than the zone center one he proposed. The intriguing question, however, is why UO_2 chooses this particular deformation? Fig. 2 shows the effect, and also suggests a possible driving mechanism. The magnetic spins lie in the (001) plane and from the ground-state wave function we know that the magnetization density is oblate (i.e., it resembles a compressed sphere with the quantization axis or dipole moment parallel to the compression axis); hence the quadrupolar electrostatic interactions are reduced with the spin configuration of Fig. 2. The spins are aligned parallel to the shortest diagonal of the parallelopiped formed by the oxygen atoms. This predicts a 2 $\vec{q}$ (or 4 sublattice) magnetic structure for UO_2, as shown in Fig. 2, rather than the single $\vec{q}$ structure assumed heretofore, but without a single domain sample neutron diffraction is unable to differentiate between these two models [14].

The studies of UO_2 with neutrons, both elastic [10,14] and inelastic [13], illustrate particularly well the power of this technique. Internal distortions, which were first predicted by Kanamori in 1960 [15], are important for our understanding of magnetoelastic interactions, and we can certainly expect them to be found in other materials in which quadrupole moments are large.

Actinide Compounds with the Rocksalt Structure

The actinide compounds with the rocksalt structure have been the subject of many investigations and, since most of them order magnetically, neutrons have played an important role in elucidating their properties. Tabulations of their various properties have appeared a number of times [1,16,17] and will not be repeated here. To a large extent their magnetic properties may be understood by assuming local moments, although the high values for the low-temperature specific heat coefficients γ (50 mJ/mole x K^2 for UN [16], for example) suggests a high density of $5f$, and possibly also $6d$, states at the Fermi level. What is not understood is the nature of the ground-state wave functions and the coupling between the moments, and four classes of neutron experiments will be described to illustrate some recent developments.

1) Magnetic Structures

Neutron diffraction has historically been the most important technique for determining the arrangement of moments in materials and has been applied to a great number of actinide systems. Among those compounds with the NaCl crystal structure the UX (X = S, Se, and Te of group VIa) are ferromagnets whereas the UX (X = N, P, As, Sb, and Bi of group Va) are simple antiferromagnets.

However, when these compounds are mixed to form pseudo-binaries, e.g., $UAs_{1-x}S_x$, then the magnetic structures become very complex, with the magnetic and crystallographic unit cells becoming incommensurate for certain compositions [18]. Long periodic structures are also found in the neptunium binary compounds and some of these are illustrated in Fig. 3 [19]. Despite the apparent complexity of these structures, there is a remarkable unifying feature, which may be stated as follows: The spin arrangements consist of ferromagnetic (001)

planes with the spin direction perpendicular to the plane, then these planes are stacked in different ways such that the $\vec{\tau}$ vector, where the repeat distance in real space is $1/\tau$, may take on a variety of values. Arrangements such as 5+,4- and 4+,3- have been reported [18]. Such a recurring theme within the structures of all antiferromagnetic uranium and neptunium compounds led to the simple concept that perhaps the coupling within the ferromagnetic planes was considerably stronger than the (presumably indirect) exchange between the planes.

2) Long-range Magnetic Correlations

When single crystals became available one of the first experiments was to search for the directional anisotropy inferred in the previous section. This is best done by studying the long-range magnetic correlations just before the material orders magnetically (i.e., in the critical regime). The crystal chosen was USb, which orders with the simple type I structure shown in Fig. 3 [20]. To visualize the experimental method we have drawn the $[1\bar{1}0]$ projection of the reciprocal lattice in the upper half of Fig. 4. Bragg points from the fcc atomic structure are (000) and (111). In principle, both (001) and (110) are magnetic points arising from magnetic domains with a [001] propagation direction. However, no Bragg peak occurs at (001) because the spin direction is then parallel to the scattering vector. Around the (001) point we should observe transverse fluctuations of the spin system in the critical region. The result of a scan from C to C' at $T_N + 3$ K is shown in the lower part of Fig. 4. No critical scattering has been observed around the (001) point, or equivalent (100) and (010) points, at any temperature. Quantitatively we can say that $\chi_T < 0.01\chi_L$, where χ_T is the transverse susceptibility and χ_L, the

longitudinal susceptibility. This is an important result, with two immediate consequences: (1) The anisotropy is considerable -- one could even argue that it defines an Ising system. (2) The critical scattering at the (110) position represents the longitudinal susceptibility directly.

At the (110) position we can perform scans in two directions. These are shown as AA' and BB' in the upper part of Fig. 4. The actual scans at (T_N + 3 K) are shown in the lower part of Fig. 4. The critical scattering is by no means isotropic around the (110) point, but shows a very diffuse nature along the direction parallel to the spin direction. Such behavior is very reminiscent of two-dimensional systems, such as K_2NiF_4, [21] in which the scattering near T_N appears in the form of rods of intensity. However, this behavior has not been observed in *cubic* materials. Similar results have been found in experiments on UN [22] but efforts to make measurements with the ferromagnets are difficult since with $\vec{\tau}$ = 0 the scattering from all domains is superimposed in reciprocal space, thus averaging any microscopic anisotropy [23].

3) Magnetic Form Factors

At first glance a neutron magnetic form factor measurement would appear to be the ideal way to resolve the question of whether the electrons are localized or itinerant, since one sees directly the spatial extent of the unpaired (i.e., magnetic) electrons. Experiments on the transition metals and compounds have shown that this is too simple an interpretati as the spin density of the wave functions near E_F is often very much like that of a free atom. In extreme cases, and perhaps $NpOs_2$ [7] is such an example, the wave functions are really delocalized, but very often a more interpretable measurement

is whether or not the form factor exhibits asphericity, in which case a deduction may often be made about the ground-state wave function.

The first experiments on US by Wedgwood [24] illustrated the difficulty in analyzing data that was essentially spherically symmetric, and we have found the same kind of form factor with recent work on the ferromagnets UTe and $USb_{0.8}Te_{0.2}$ [25]. In contrast, the form factor of USb [26] showed considerable anisotropy. A detailed analysis in terms of possible crystal-field states led to the assignment of a $5f^3$ configuration with a wave function dominated by the M = |7/2> component. Our expectation, based on crystal-field arguments as well as the analogous lanthanide compound NdSb [27], had been for a ground state wave function consisting primarily of the |M = 9/2> component, which has a prolate distribution of magnetization density about the ordered moment. Instead, in USb the magnetization density is definitely oblate in shape, and we show this schematically in Fig. 5. Here we also give a conceptual picture of the *f*-*p* hybridization that has been advanced [28] to understand the nature of the ground-state wave functions and why the very large difference occurs between the interactions within the ordered (001) planes and between them, as discussed in the previous section. However, the more quantitative predictions of this idea have still to emerge.

In uranium compounds the free-atom form factors of the $5f^2$ and $5f^3$ configurations look almost identical [29], so that to obtain useful information we have concentrated on the aspherical features, where they exist. For transuranium systems, on the other hand, the general shape of the form factor may be able to give unambiguous information. This is particularly true in the case of plutonium in its trivalent state, in which case (as with Sm^{3+}) $\vec{J} = \vec{L} - \vec{S}$

and $\vec{L}$ (= 5) and $\vec{S}$ (= 5/2) partially cancel. In Fig. 6 we show the magnetic form factor as measured in two ferromagnets PuP and $PuFe_2$ [30], both measurements were performed with polarized neutrons on polycrystalline samples. The remarkable flatness of the form factor out to high scattering angles is because the total magnetization density has a negative region in real space. Such an unusual form factor allows us immediately to assign the trivalent ionization state to these compounds, and in the case of PuP we were also able to give an upper limit to the extent of J mixing. This was considerably less than previously thought, making the neutron experiment doubly useful.

4) Crystal-field Levels and Collective Excitations

The measurement of the elementary magnetic excitations by neutron inelastic scattering provides detailed information about the ground and excited state wave functions and the nature, strength, and possible anisotropy of the exchange interactions. On metallic actinide systems the first experiments were performed on polycrystalline UX samples by Wedgwood [31]. In view of the importance of the crystal-field interactions it was therefore surprising that no sign of any discrete crystal-field levels were found with neutron spectroscopy. The investigations on polycrystalline samples should be able to see dispersionless exciton levels, but cannot hope to measure collective excitations, which are at discrete position in $\vec{Q},\omega$ space. For these studies large ($\geq$ 2 g) single crystals are needed. The first experiments on UN, however, provided even greater mysteries since no discrete excitations at all were seen [22]. More recently, poorly defined excitations have been seen in UN near the magnetic zone center, and this work is continuing at Chalk River with the first experiments on ferromagnet UTe [32].

A rather detailed examination of the collective excitations has now been performed at the Institut Laue Langevin on USb and we reproduce the dispersion curves in Fig. 7 [33]. The most surprising features are: (a) The observation of a longitudinally polarized mode at low frequency, i.e., a modulation of the *size* of the magnetic moment along the quantization axis, rather than a conventional spin wave, which corresponds to the precession of the magnetic moments about the quantization axis. (b) At the magnetic zone center, X point (110), the collective magnetic excitation has the same frequency as the phonon. (c) As the temperature is raised the amplitude of this collective excitation rapidly decreases and is essentially unobservable above $T_N/2$. Further details of these rather long and complex experiments are beyond the scope of the present article; suffice it to say that models based on lanthanide type of behavior are quite unable to account for these results, so we have a very exciting situation where we can anticipate both new experiments and (hopefully) greater attention from the theorists.

Discussion

No mention has been made in this article of neutron methods, formulae, or technology. As one would expect, the techniques developed for other elements and compounds of the periodic table have proved their worth in actinide investigations, and the references contain full details. Our aim has been to address the question of what makes the actinides so interesting from the viewpoint of a solid-state physicist, and why neutron scattering is such an important tool in these studies. The special advantages of neutron scattering include: (a) The penetrating power of the neutron, thus making encapsulation relatively easy for active samples. (b) The sensitivity

to light atoms in the presence of heavy ones, and examples range from the early identification that UN had the rocksalt structure [34] to the measurement of the lattice dynamics [35] and the internal distortion [14] in UO_2. (c) From the interaction of the neutron with the magnetic moments we are able to deduce magnetic structures, the value of the localized magnetic moment, the shape of the $5f$ electron wave functions, and the extent of the magnetic correlations. We can also use the extreme sensitivity of the polarized-neutron technique to measure the induced magnetic moment (as small as 0.01 μ_B) in paramagnetic systems, and determine the spatial extent of this induced magnetization throughout the unit cell [36]. These measurements are of particular interest since they can be compared with theoretical spin densities, and thus form the basis for a rigorous test of the eigenfunctions used in fitting the de Haas van Alphen frequencies [37]. (d) From the fact that neutrons have energies close to those of elementary excitations (0.01 - 0.1 eV) we are able to measure phonons [35] and study the dynamics of phase transitions [3]. Combining the magnetic interaction with inelastic scattering we can search for crystal-field levels, measure the collective magnetic excitations, and the generalized magnetic response function $S(\vec{Q},\omega)$. This latter measurement tells us something abou the spin dynamics and whether such materials as UAl_2 can be assigned a distinct $5f$ electron configuration [38].

The dominance of *magnetic* interactions is for a good reason. It is the unpaired $5f$ electrons that give the actinides and their compounds such a variety of properties, and by utilizing the magnetic interaction we have a probe that selects out the very unpaired electrons of greatest interest.

There are additional areas that are now being explored, but which space does not permit us to discuss, e.g., a search for a possible internal distortion in NpO_2, a search for paramagnon fluctuations in UAl_2, uniaxial stress measurements on UN and UAs, high field studies (>90 kOe) of the magnetic phase transitions in UAs, the study of complex magnetic structures with single crystals, and polarization analysis experiments on PuP to search for the conduction-electron polarization.

The greatest *disadvantage* of neutron scattering is that the fluxes are low and the interactions are weak. We therefore often need large samples. Within the foreseeable future we cannot expect much respite from this requirement, especially as we turn to more and more complex neutron technology to solve the physics. However, the ability to produce single crystals of uranium compounds augurs well for the future of this field, since the chemistry and metallurgy of the first few actinide elements and their compounds are not substantially different. To obtain single crystals of transuranium compounds, and thus realize the full potential of neutron scattering, presents great difficulties, but a rich harvest certainly awaits those Laboratories willing to accept the challenge.

Acknowledgments

The production of single crystals of uranium compounds has proved the key to many of the new developments discussed above, and I am particularly indebted to Oscar Vogt of ETH, Zurich for the major role he has played in this field. I should like to record my thanks for collaboration and discussions with A. J. Arko, P. J. Brown, W. J. L. Buyers, B. R. Cooper, A. Delapalme, A. J. Freeman, T. M. Holden, J. F. Reddy, J. Rossat-Mignod, S. K. Sinha, W. G. Stirling and H. G. Smith.

References

* Work supported by the U. S. Department of Energy.

[1] "The Actinides: Electronic Structure and Related Properties", A. J. Freeman and J. B. Darby, ed. (Academic Press, N.Y. 1974) vol. I and II. M. B. Brodsky, Rep. Progr. Physics. 41 (1978) 1547.

[2] W. P. Crummett, H. G. Smith, R. M. Nicklow, and N. Wakabayashi, Phys. Rev. B (in press).

[3] H. G. Smith, N. Wakabayashi, W. P. Crummett, R. M. Nicklow, G. H. Lander and E. S. Fisher, to be published in AIP Conf. Proc. as Proceedings of Conference on modulated structures, Hawaii, March, 1979.

[4] J. M. Fournier, A. Blaise, W. Muller and J. C. Spirlet, Physica 86-88B (1977) 30.

[5] H. Hill, in "Plutonium and other Actinides," W. N. Miner, ed. (AIME, New York, 1971) p. 2.

[6] A. T. Aldred, B. D. Dunlap, D. J. Lam and I. Nowik, Phys. Rev. B 10 (1974) 1011; B 11 (1975) 530.

[7] A. T. Aldred, B. D. Dunlap and G. H. Lander, Phys. Rev. B 14 (1976) 1276.

[8] B. D. Dunlap and G. H. Lander, Phys. Rev. Letters 33 (1974) 1046

[9] M. B. Brodsky and R. J. Trainor, Physica 91B (1977) 271.

[10] B. C. Frazer, G. Shirane, D. E. Cox and C. E. Olsen, Phys. Rev. 140 (1965) A1448.

[11] H. U. Rahman and W. A. Runciman, J. Phys. Chem. Solids 27 (1966) 1833; 30 (1969) 2497; H. U. Rahman, Physica 45 (1970) 511.

[12] S. J. Allen, Phys. Rev. 166 (1968) 530; 167 (1968) 492.

[13] R. A. Cowley and G. Dolling, Phys. Rev. 167 (1968) 464; Phys. Rev. Letters 16 (1966) 683.

[14] J. Faber and G. H. Lander,Phys. Rev. B 14 (1976) 1151; Phys. Rev. Letters 35 (1975) 1770.

[15] J. Kanamori, J. Appl. Physics 31 (1960) 14S.

[16] J. Grunzweig-Genossar, M. Kuznietz and F. Friedman, Phys. Rev. 173 (1968) 562.

[17] G. H. Lander, Inst. Physics (London) Conf. Series 37 (1978) 173.

[18] M. Kuznietz, G. H. Lander and Y. Baskin, J. Appl. Physics 40 (1969) 1130; Phys. Rev. 188 (1969) 963; J. Leciejewicz, A. Murasik, R. Troc, and T. Palewski, Phys. Stat. Solidi 46 (1971) 391; G. H. Lander, M. H. Mueller and J. F. Reddy, Phys. Rev. B 6 (1972) 1880.

[19] A. T. Aldred, B. D. Dunlap, A. R. Harvey, D. J. Lam, G. H. Lander and M. H. Mueller, Phys. Rev. B 9 (1974) 3766.

[20] G. H. Lander, S. K. Sinha, D. M. Sparlin and O. Vogt, Phys. Rev. Letters 40 (1978) 523.

[21] R. J. Birgeneau, J. Skalyo and G. Shirane, Phys. Rev. B 3 (1971) 1736; J. Appl. Phys. 41 (1970) 1303.

[22] W. J. L. Buyers, T. M. Holden, E. C. Svensson and G. H. Lander in "Proc. of Int. Symposium on Neutron Inelastic Scattering (Int. Atomic Energy Agency, Vienna, 1978) p. 239.

[23] H. Bjerrum-Møller, G. H. Lander and O. Vogt, J. de Physique 40 (1979) C4-28.

[24] F. A. Wedgwood, J. Phys. C 5 (1972) 2427.

[25] G. Busch, O. Vogt, A. Delapalme and G. H. Lander, J. Phys. C 12 (1979) 1391.

[26] G. H. Lander, M. H. Mueller, D. M. Sparlin and O. Vogt, Phys. Rev. B 14 (1976) 5035.

[27] A. Furrer, W. J. L. Buyers, R. M. Nicklow and O. Vogt, Phys. Rev. B 14 (1976) 179.

[28] S. K. Sinha and A. J. Fedro, J. de Physique 40 (1979) C4-214.

[29] A. J. Freeman, J. P. Desclaux, G. H. Lander and J. Faber, Phys. Rev. B 13 (1976) 1168; J. P. Desclaux and A. J. Freeman, J. Magn. & Mag. Matls. 8 (1978) 119.

[30] PuP: G. H. Lander and D. J. Lam, Phys. Rev. B 14 (1976) 4064

$PuFe_2$: G. H. Lander, A. T. Aldred, B. D. Dunlap and G. K. Shenoy, Physica 86-88B (1977) 152.

[31] F. A. Wedgwood, J. Phys. C 7 (1974) 3203.

[32] W. J. L. Buyers, A. F. Murray, E. C. Svensson, T. M. Holden, P. du Plessis, G. H. Lander and O. Vogt, submitted to Int. Conf. on "Neutron Scattering and Magnetism", Julich, August 1979, to be published in J. Mag. & Mag. Matls.

[33] G. H. Lander, W. G. Stirling and O. Vogt, Phys. Rev. Letters 42 (1979) 260; Phys. Rev. (to be published).

[34] M. H. Mueller and H. W. Knott, Acta Crystallogr. 11 (1958) 751.

[35] G. Dolling, A. D. B. Woods and R. A. Cowley, Can. J. Phys. 43 (1965) 1397.

[36] URh_3: A. Delapalme, G. H. Lander and P. J. Brown, J. Phys. C 11 (1978) 1441;

α-U: R. C. Maglic, G. H. Lander, M. H. Mueller and R. Kleb, Phys. Rev. B 17 (1978) 308;

UGe_3: G. H. Lander, J. F. Reddy, A. Delapalme and P. J. Brown, see Proceedings as in Ref. [32].

[37] URh_3: A. J. Arko, M. B. Brodsky, G. W. Crabtree, D. Karim, D. D. Koelling, L. R. Windmiller and J. B. Ketterson, Phys. Rev. B 12 (1975) 4102.

UGe_3: A. J. Arko and D. D. Koelling, Phys. Rev. B 17 (1978) 3104.

[38] M. Loewenhaupt, S. Horn, F. Steglich, E. Holland-Moritz and G. H. Lander, J. de Physique 40 (1979) C4-12.

Figure Captions

Fig. 1. Linear relationship between the hyperfine field H_{hf} and the magnetic moment μ_N in neptunium intermetallics. Experimental points are shown by closed circles and calculated free-ion values by open circles [8]. MSD Neg. No. 61887.

Fig. 2. (001) projection of the fluorite structure. The closed and open circles represent uranium atoms at z = 0 and z = 1/2, respectively. The large circles represent oxygen atoms at z = 1/4 and z = 3/4 displaced from the ideal fluorite lattice (indicated by the dashed lines). The shift of the oxygen atoms is not drawn to scale, $\Delta/a = 2.6 \times 10^{-3}$. The suggested noncollinear spin configuration is also shown. MSD Neg. No. 61835.

Fig. 3. Magnetic structures of NpX compounds [19]. NpN is a ferromagnet with a <111> easy axis. NpP has a sinusoidal modulation of the magnetic moment along the propagation axis with a repeat of 3 unit cells, 6 (001) planes. At high temperature, NpAs has a 4+, 4-, structure but has a first-order transition at 142 K to the type-I, +-, structure, which is also the structure of NpSb.
ANL Neg. No.

Fig. 4. Measurement of long-range magnetic correlations in USb [20]. Upper section, $[1\bar{1}0]$ projection of the reciprocal lattice. Lower section, experimental points and least-squares fits (solid lines) for the scans as shown in the upper section. The small bars indicate the experimental resolution functions.
MSD Neg. Nos. 62919 and 64680.

Fig. 5. This shows schematically the oblate magnetization density [26] at the uranium sites (solid circles) and the proposed overlap of the anion (open circles) p wavefunctions [28]. Notice that because the $5f$ wave function is extended in the (001) plane the overlap is much stronger in this plane than between the planes.

Fig. 6. Magnetic form factors of Pu^{3+}. Upper curve, results for PuP [30]. The solid and dashed curves are the best fits to the data with $5f^5$ and $5f^4$ configurations, respectively. The arrow on the ordinate axis gives the total moment determined by magnetization experiments, the discrepancy of $\sim 0.3\ \mu_B$ between this and the neutron experiment being due to conduction-electron polarization. The insert shows the relativistic Dirac-Fock values for $\langle j_0 \rangle$ and $\langle j_2 \rangle$, see Ref. [29]. The lower figures are form factors measured in $PuFe_2$ [30]. Notice that, although the Pu moment is $\sim 0.4\ \mu_B$ as compared to $1.4\ \mu_B$ for the iron moment, at high angles the scattering is dominated by the Pu moment because of the unusual Pu^{3+} form factor.

Fig. 7. The dispersion curves for USb [33]; energy plotted against wave-vector transfer $\vec{Q}$ (in units of $2\pi/a$). The dashed lines represent the phonons with the open points as measurements. The solid points are the longitudinally polarized collective excitation with a 1.5 THz (= 6.2 meV) anisotropy gap at the zone center (X point). A dispersionless (and temperature independent) exciton, which is probably a crystal-field level, is located at ~ 6.5 THz (= 27 meV) and indicated by the hatched area.

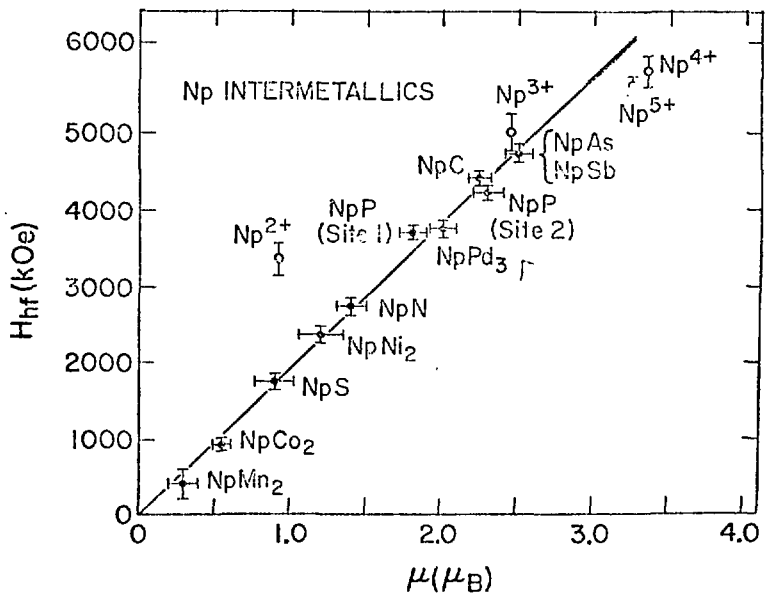

Fig. 1. Linear relationship between the hyperfine field H_{hf} and the magnetic moment μ_N in neptunium intermetallics. Experimental points are shown by closed circles and calculated free-ion values by open circles . [8]

MSD Neg. No. 61887

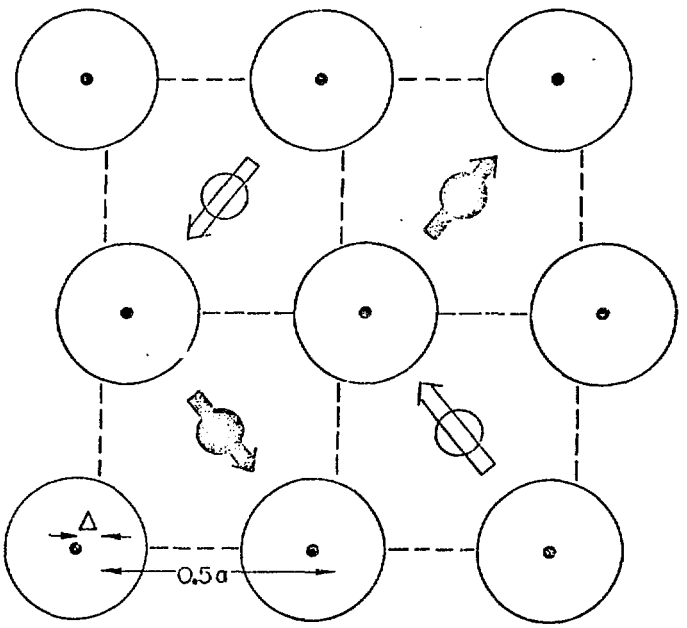

Fig. 2. (001) projection of the fluorite structure. The closed and open circles represent uranium atoms at z = 0 and z = 1/2, respectively. The large circles represent oxygen atoms at z = 1/4 and z = 3/4 displaced from the ideal fluorite lattice (indicated by the dashed lines). The shift of the oxygen atoms is not drawn to scale, $\Delta/a = 2.6 \times 10^{-3}$. The suggested noncollinear spin configuration is also shown.

MSD Neg. No. 61835.

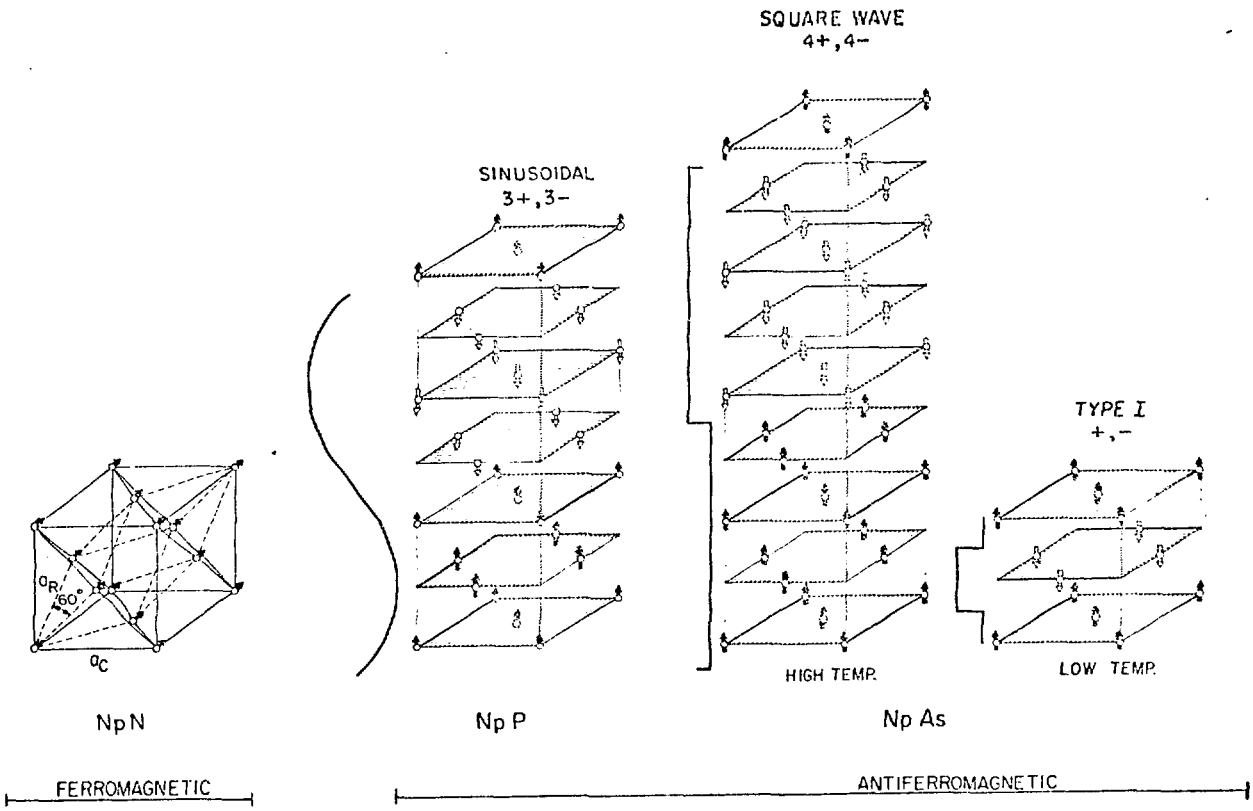

Fig. 3. Magnetic structures of NpX compounds [19]. NpN is a ferromagnet with a <111> easy axis. NpP has a sinusoidal modulation of the magnetic moment along the propagation axis with a repeat of 3 unit cells, 6 (001) planes. At high temperature, NpAs has a 4+, 4-, structure but has a first-order transition at 142 K to the type-I, +-, structure, which is also the structure of NpSb.

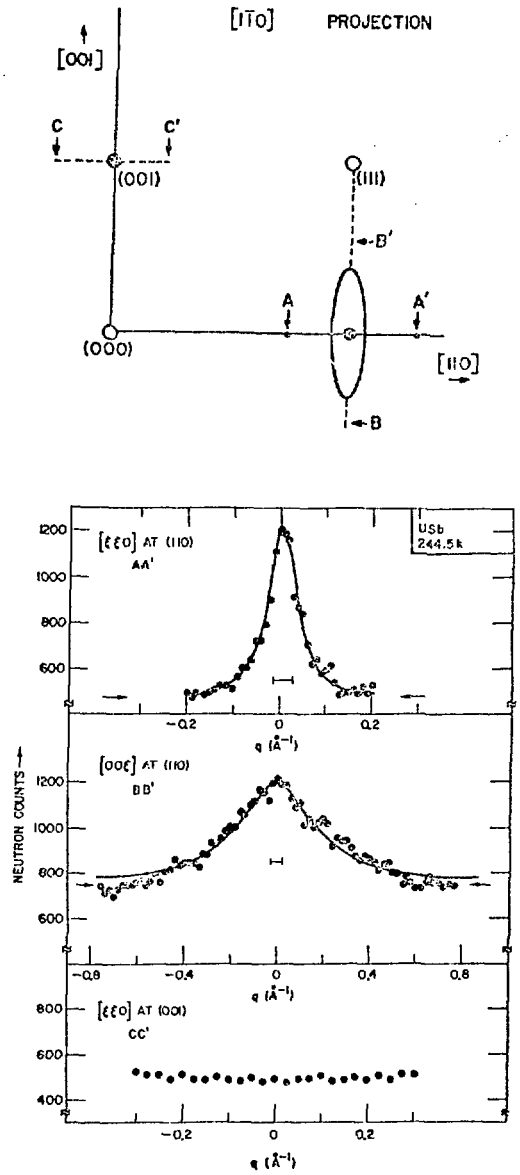

Fig. 4. Measurement of long-range magnetic correlations in USb [20]. Upper section, [1$\bar{1}$0] projection of the reciprocal lattice. Lower section, experimental points and least-squares fits (solid lines) for the scans as shown in the upper section. The small bars indicate the experimental resolution functions.

MSD Neg. Nos. 62919 and 64680.

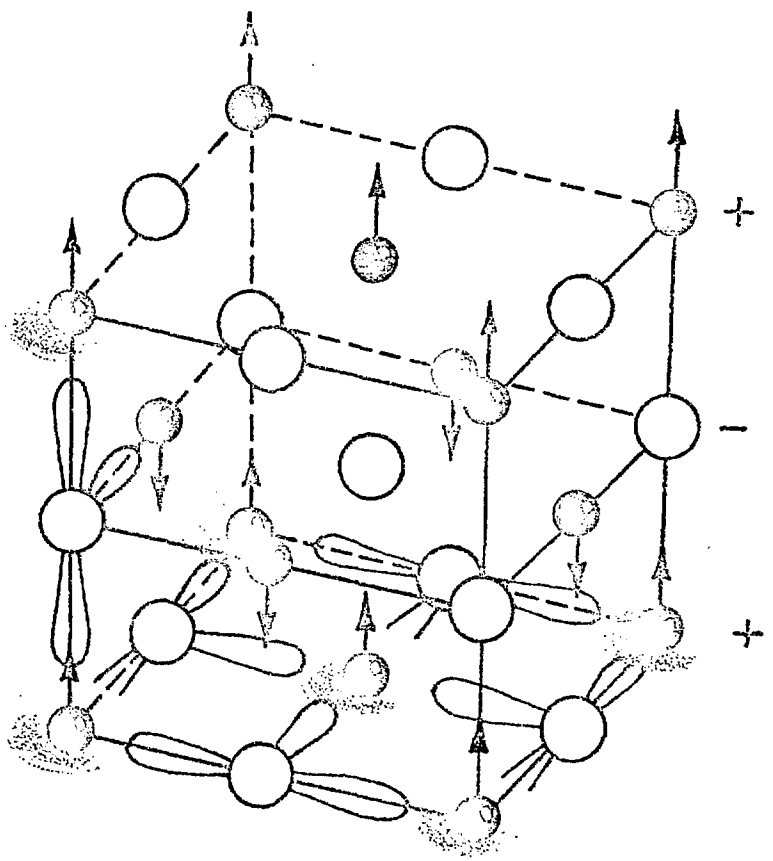

Fig. 5. This shows schematically the oblate magnetization density [26] at the uranium sites (solid circles) and the proposed overlap of the anion (open circles) p wavefunctions [28]. Notice that because the $5f$ wave function is extended in the (001) plane the overlap is much stronger in this plane than between the planes.

Figure 6.
Magnetic form factors of Pu^{3+}. Upper curve, results for PuP [30]. The solid and dashed curves are the best fits to the data with $5f^4$ and $5f^4$ configurations, respectively. The arrow on the ordinate axis gives the total moment determined by magnetization experiments, the discrepancy of $\sim 0.3\ \mu_B$ between this and the neutron experiment being due to conduction-electron polarization. The insert shows the relativistic Dirac-Fock values for $\langle j_0 \rangle$ and $\langle j_2 \rangle$, see Ref. [29]. The lower figures are form factors measured in $PuFe_2$ [30]. Notice that, although the Pu moment is $\sim 0.4\ \mu_B$ as compared to $1.4\ \mu_B$ for the iron moment, at high angles the scattering is dominated by the Pu moment because of the unusual Pu^{3+} form factor.

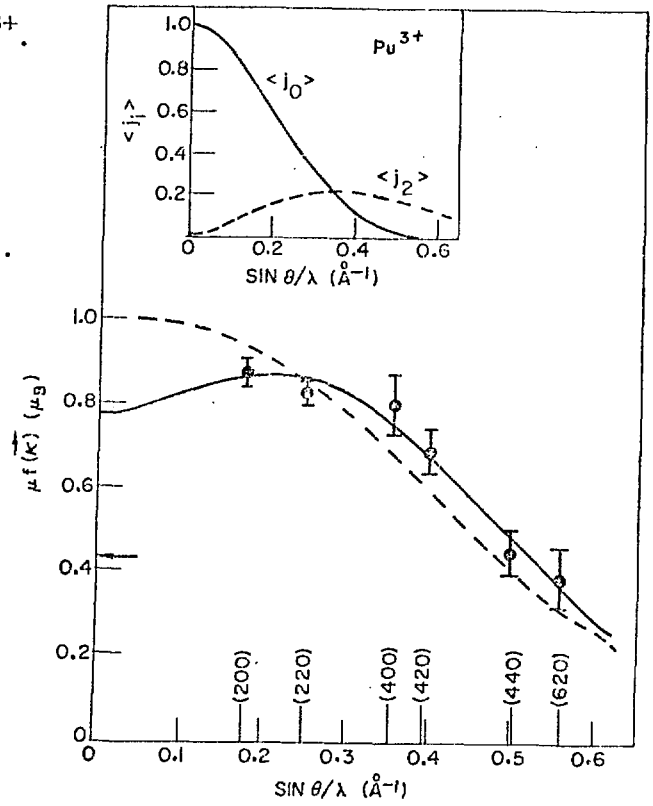

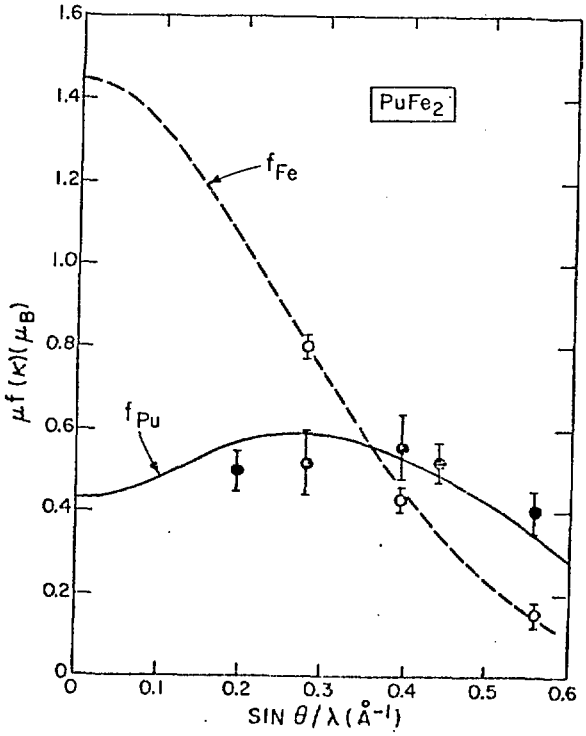

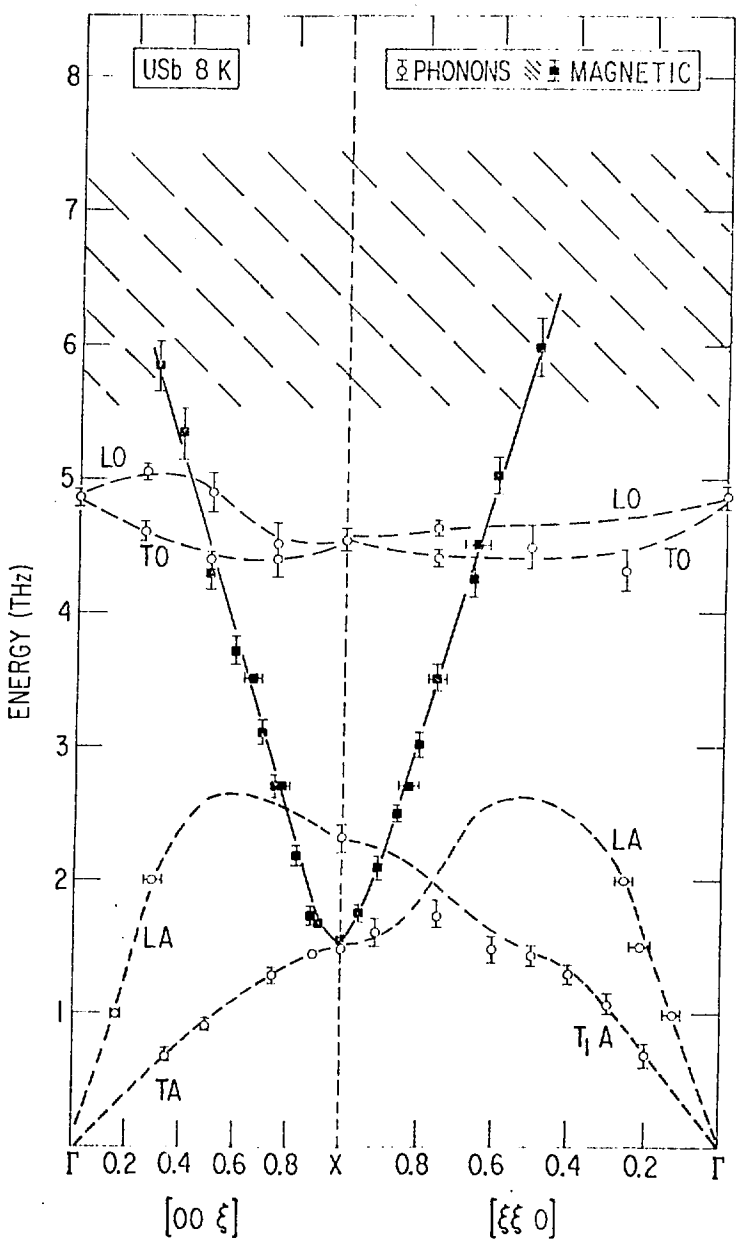

Fig. 7. The dispersion curves for USb [33]; energy plotted against wave-vector transfer $\vec{Q}$ (in units of $2\pi/a$). The dashed lines represent the phonons with the open points as measurements. The solid points are the longitudinally polarized collective excitation with a 1.5 THz (= 6.2 meV) anisotropy gap at the zone center (X point). A dispersionless (and temperature independent) exciton, which is probably a crystal-field level, is located at ∿6.5 THz (+ 27 meV) and indicated by the hatched area.